doi:10.14311/ppt.2025.2.112
Plasma Physics and Technology **12**(2):112–116, 2025

MODELLING OF MICRODISCHARGES IN METAL VAPOUR OF CADMIUM IN COMPARISON WITH ELECTRICAL MEASUREMENTS

M. Baeva[a,*], A. P. Jovanović[a], R. Methling[a], D. Bratek[b], N. Schüler[b], C. Uber[b], D. Uhrlandt[a]

[a] *Leibniz Institute for Plasma Science and Technology, 17489 Greifswald, Germany*

[b] *Physikalisch-Technische Bundesanstalt (PTB), Bundesallee 100, 38116 Braunschweig, Germany*

[*] baeva@inp-greifswald.de

Abstract. Microdischarges in cadmium vapour occur in a testing equipment for safety assessment of electric devices for explosion protection. In this work, a unified non-equilibrium model is employed to obtain the plasma properties for a current of 60 mA and gap lengths from 20 up to 160 µm corresponding to conducted experiments. The predicted voltage as a function of the discharge length agrees well with the measured values. The model provides the heat generation relevant to the ignition of a gas mixture.

Keywords: microdischarge, fluid model, cadmium, safety assessment.

1. Introduction

Explosion protection is a critical concern for various industrial fields where flammable gases are used. The risk of gas ignition due to the triggering of electric discharges at low voltages and currents during routine operations (such as plugging and unplugging of the equipment or the contact opening) raises interest in these types of discharges and test devices were constructed to study them (see e.g., [1, 2] and the references therein). The gas ignition by these discharges was first noticed at higher voltages and currents and later observed for lower currents in the range of 30 mA. During the contact opening, a microdischarge starts in metal vapour released from the cathode surface. It causes heating in the plasma, the electrodes, and the surrounding gas.

Recent experimental studies of contact discharges [1–3] showed that the process undergoes four phases. First, an electric contact of a wire (anode) is established on the rough surface of a metal block (cathode). Second, the wire is pulled away from the surface which initiates an electric discharge. Third, the main discharge develops in metal vapour at distances between 20 µm and ∼ 200 µm (the so-called microdischarges). Fourth, the wire moves further away from the surface, the released heat causes a thermochemical reaction, which can lead to the formation and the development of a flame front. An empirical discharge model was employed to investigate the transient electric discharge at low voltage and predict the voltage and current waveforms, and the gas heating in [4]. This model differs therefore from models like that reported in [5], in which time-dependent transport equations for all charged and neutral species and Poisson's equation are solved.

In this work, we present a study of the discharge development in the metal vapour with the emphasis on the characterization of the plasma based on a time-dependent, spatially one-dimensional (1D) unified non-equilibrium discharge model for air plasma dominated by copper metal vapour [6]. The understanding of the underlying processes in the contact microdischarge and the validation of the model in metal vapour of cadmium by means of electrical measurements are the main objectives. The determination of the gas heating is crucial in identifying the condition at which the flammable gas can be ignited. The parameters obtained for a cadmium vapour plasma represent the main novel aspects of the work.

2. Summary of the model

The 1D unified non-equilibrium model employed in this study is described for the case of microarcs between copper electrodes in the recent work [6]. Here, the adoption of the model is explained in more detail. The schematic of the discharge follows the experimental arrangement and is shown in figure 1a. The model considers a cathode made of cadmium (Cd) and an anode made of tungsten (W) with lengths of 10 mm and a diameter of 100 μm each. The length of the plasma region varies from 20 μm up to 160 μm during the contact separation. Figure 1b shows the external circuit with a voltage source U_0 and a ballast resistor R_b used in the model for the regulation of the electric current. The plasma is assumed to contain electrons and heavy particles of Cd atoms and singly charged Cd^+ ions in their ground states. Analogous to the model in [6], the contribution of excited Cd atoms to the electron impact ionisation is taken into account applying the modified diffusion approximation (MDA) [7]. An introduction of excited states will be pursued in a forthcoming work. The electrons are characterized by a Maxwellian velocity distribution function with a temperature T_e, while the heavy species are assumed in equilibrium at a common temperature T. The emission of electrons from the non-refractory Cd cathode

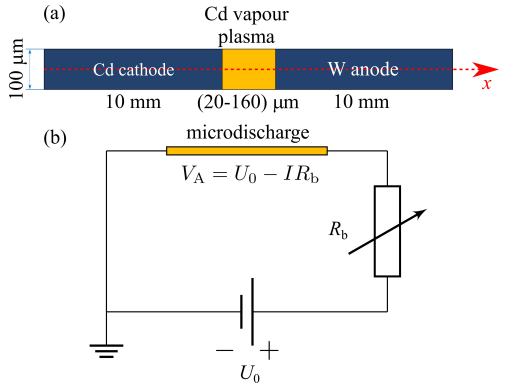

Figure 1. Schematic of the discharge arrangement (a) and equivalent circuit (b) used in the model.

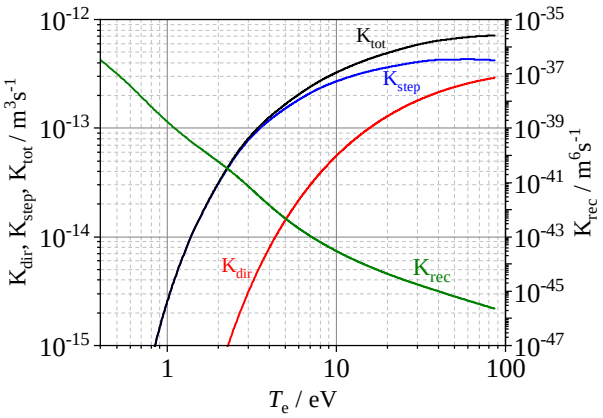

Figure 2. Rate coefficients of direct K_{dir}, step-wise K_{step}, and total ionisation K_{tot} of Cd atoms, and 3-body recombination K_{rec} as a function of T_e.

is evaluated as a thermo-field emission and computed following [8]. A secondary electron emission due to ion bombardment on the cathode is taken into account with a coefficient of 0.07 because of lack of data for Cd. Note that the secondary electron emission is negligible in the problem under consideration and is included for the sake of completeness. Figure 2 shows ionisation coefficients (left-hand side scale) and recombination coefficient (right-hand side scale) as a function of T_e computed according to the MDA [7]. Note that due to the low ionisation potential of Cd (8.99 eV), the contribution of the low-lying excited states of the Cd atoms is appreciable. For T_e in the range (1-4) eV, the total ionisation rate coefficient equals that for a step-wise ionisation. The MDA allows one to account for the contribution of the excited states and to reduce the number of species in the model.

A pre-computed electron emission current density is provided as a function of the electric field and the temperature at the cathode surface (see Figure 3). The computation applies the Transferred Matrix Method and is described in detail in [8]. The particular behaviour indicates that current densities in the order of 10^6 Am^{-2} can be reached for a magnitude of the electric field in the order of 10^9 Vm^{-1}. The typical values in the 1D model are, however, in the order 10^7 Vm^{-1}. Therefore, a field enhancement factor (FEF) is introduced to account for surface roughness and protrusions [6], that can locally increase the electric field. A derivation of the field enhancement factor accounting for the surface roughness is out of scope of the 1D model. In general, such considerations are done for some materials. Values for polished copper can locally reach 200 to 500 [9]. Here, the FEF multiplies the electric field obtained from the Poisson's equation to find an effective electric field for which the emission current density is taken.

The governing equations for the particle and energy transport as well as the heat transfer in the electrodes are analogous to equations (1)–(11) in [6]. The material properties of Cd (vapour, solid, liquid) used in the model are as follows. The thermodynamic parameters of Cd and Cd^+ (heat capacity, enthalpy) are temperature-dependent and prepared as look-up tables for temperatures up to 20000 K [10], the diffusion coefficients of the species in the mixture are computed by the binary diffusion coefficients in terms of the kinetic gas theory. The mobility of the ions is expressed by the Einstein relation with common temperature T. The transport of heavy species is in part readily implemented in the computational platform COMSOL Multiphysics ®. The properties of the electrodes are taken from [11, 12]. The data for the vapour pressure is from [13]. The cross-section data for elastic collisions and ionisation by electron impact is from [14].

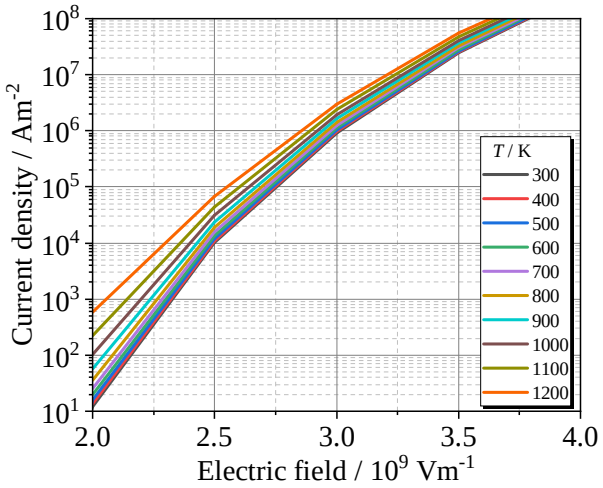

Figure 3. Thermo-field emission current density of electrons as a function of the electric field and temperature at the cathode surface.

3. Electrical measurements

The electrical characteristics of the discharge have been studied and quasi-stationary current-voltage characteristics have been obtained by using a setup that includes a DC control system, oscilloscope, providing the electrical parameters with a time step of

1.6 μs, long distance microscope, image intensifier, and a high-speed camera (for further details, see [1]).

The discharge length is measured along the line connecting the strongly emitting anode and cathode areas. The length is defined as the distance between the endpoints, which represent the half of the maximum emission intensity. The discharge width is taken along lines that are perpendicular to the central line. Here again, the value at the half-maximum of the emission intensity is considered. Over 600 measurements for 15 discharges were carried out with a current of 60 mA and reported in previous works (see e.g., [1]).

4. Results and discussion

The model equations are solved using a fully coupled approach. The plasma domain is resolved in 1600 mesh elements and 300 elements are used for the electrodes. The initial time step is 1×10^{-13} s. An automated increase is enabled in case the convergence criteria are satisfied. The electric current in the model has a constant value of 60 mA. A steady-state solution is sought for a gap length of 20 µm to mimic the initial two phases of contact opening. Then, a deforming mesh approach is applied to simulate the moving electrode. The discharge gap was increased from 20 µm up to 160 µm with a speed of 0.14 m/s. Results are obtained for various FEF. The predicted voltage as a function of the discharge length was compared with the experimental results (see Figure 4). Due to the stochastic nature of the electric breakdown and unstable conditions during the contact opening, the measured data are quite scattered. This effect cannot be captured by the model. Moreover, the variation of the FEF leads to various arc voltage values in the model. The predicted voltage decreases with the increase of FEF. This behaviour is related to the increase of the thermo-field current density and cooling of the cathode. A discussion of the heat flux components on the electrodes can be found in [6]. For a given FEF, the model reproduces the linear dependence of the voltage on the discharge length observed in the experiment. For FEF of 140, the modelling results correspond to the mean experimental values. Further results are presented for this FEF. The results are presented for discrete time intervals corresponding to lengths ranging from 20 µm up to 160 µm.

Figure 5 shows the distributions of the electron and ion number densities during the contact opening. The results show that a quasi-neutral plasma bulk occupies the most of the discharge gap. The region of space charge adjacent to the cathode has a length of about 2 µm and is dominated by Cd^+ ions. The peak value of the charge carrier densities increases slightly and shifts away from the cathode during the contact opening for gap lengths up to about 100 µm. This behaviour suggests that an increase in voltage compensates for the change in the discharge length. This can be explained as follows. Once the cathode and anode falls are built, the remaining voltage over the plasma bulk drops linearly. This results in an almost constant electric field determined by the balance of the processes of charge production and loss. The increase of the length of the microdischarge effectively extends this plasma region [15]. In order to maintain this balance and the quasi-neutral plasma bulk, the electric potential at the anode, and the discharge voltage, respectively, has to increase.

Figure 6 displays the spatial distribution of the electric potential and electric field in the discharge gap during the contact opening. Note that the graph contains the results for gap lengths from 20 up to 160 µm with a step of 20 µm. The cathode fall that amounts to approx. 15 V is followed by an almost linear voltage increase towards the anode, and a positive anode fall (the increase of the electric potential and the electric field in the vicinity of the anode can be clearly seen for the various gap lengths). The electric field is less than 10^5 Vm^{-1} in the plasma bulk but strongly increases to about 2×10^7 Vm^{-1} and 10^6 Vm^{-1} in the vicinity of the cathode and the anode, respectively. Note that the behaviour of the electric potential indicates no reversal of the electric field unlikely to microarcs in gases [6].

Figure 7 shows T and T_e in the discharge gap during the contact opening. The results for gap lengths from 20 up to 160 µm with a step of 20 µm are shown. A field enhancement factor of 140 is used in the computation. The Joule heating is the main mechanism for the heating of the gas and electrons. It is caused respectively by the ion and electron components of the electric current density. Elastic collisions between electrons and heavy species represent a loss term for the density of electron energy and a heating term for the heavy particles. For small gap lengths, the gas temperature T is highest close to the anode, while its peak value shifts towards the middle of the gap for longer distances. This behaviour results from the

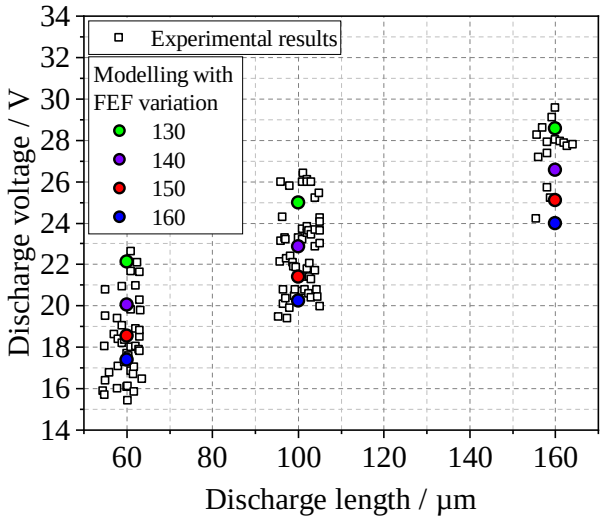

Figure 4. Predicted and measured voltage as a function of the discharge length for various FEFs.

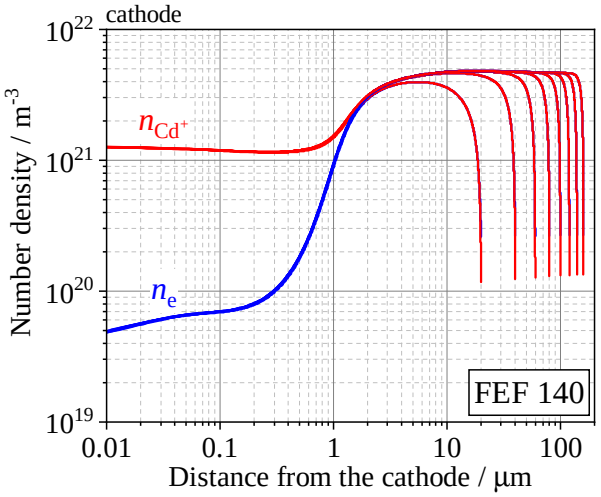

Figure 5. Number density of electrons and Cd^+ ions during the contact opening. The graph contains the results for gap lengths from 20 up to 160 µm with a step of 20 µm. The results are obtained with a value of the field enhancement factor FEF=140.

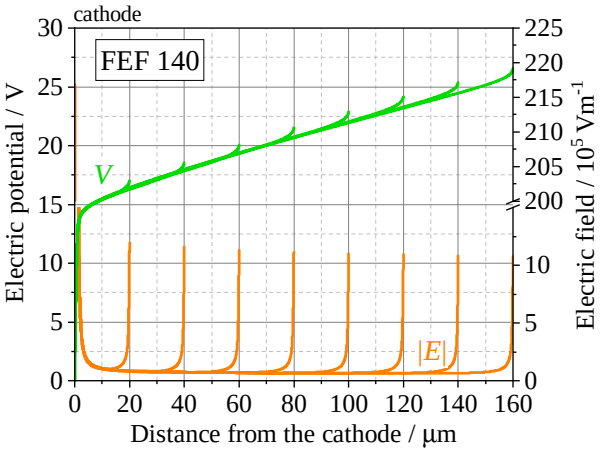

Figure 6. The electric potential (left axis) and electric field (right axis) in the discharge gap during the contact opening. The graph contains the results for gap lengths from 20 up to 160 µm with a step of 20 µm. The results are obtained with a value of the field enhancement factor FEF=140.

interplay of the volumetric heating of the gas and the heat transfer in the anode. On the boundary between the plasma and the anode, a heat flux from the plasma adds up the term due to heat conduction. At a distance of 120 μm, T approaches a maximum value of about 3000 K, is well above the ignition temperature of the H_2-air mixtures. The results clearly show that the plasma is in thermal non-equilibrium, which is in agreement with experiments [3]. The model predicts T_e-values of about 5000 K in the bulk plasma, and about 20000 K and 8000 K in the vicinity of the cathode and the anode, respectively.

Modelling results further show that the temperature on the cathode end that is in contact with the plasma remains almost constant at a value of ~950 K, while

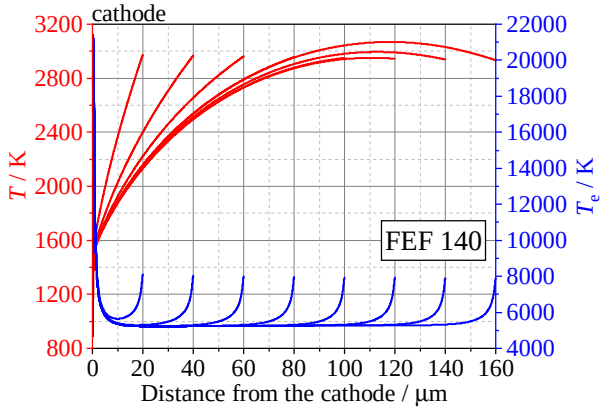

Figure 7. Spatial distributions of the gas (T) and electron (T_e) temperatures in the discharge gap during the contact opening. The graph contains the results for gap lengths from 20 up to 160 µm with a step of 20 µm. The results are obtained with a value of the field enhancement factor FEF=140.

the anode temperature slightly decreases during the contact opening. The evaluation of the heating fluxes (see equations 12 and 13 in [6]) on the electrodes show that the cathode is mainly heated by the ion flux and cooled by evaporation. The anode is mainly heated by electron condensation.

5. Conclusions

This work was focused on modelling of microdischarges in Cd metal vapour during the contact separation and the comparison of the model predictions with results from electrical measurements. The main results can be summarised as follows.

- The comparison of the model predictions with the measured voltage allows us to calibrate the model with respect to the conditions for the electron emission regime of the cathode made of Cd. The results obtained show a good agreement with the experiment for values of the FEF of 130-160. For these values, the predicted voltage as a function of the discharge length agrees with the statistically spread experimental values.
- Plasma parameters are obtained and presented in detail for FEF of 140. They show the temporal and spatial development of the discharge during the contact opening.
- The results indicate the thermal non-equilibrium of the plasma over the entire discharge length.
- The spatial extent and the values of the voltage drop in the regions of the cathode and anode space charge sheaths are obtained.

Forthcoming works will focus on modelling and experiments of the plasma emission by means of introduction of excited states in the model and optical emission spectroscopy.

6. Data availability statement

The data that support this study are openly available at the following URL/DOI: www.inptdat.de/dataset/Modelling-studies-of-arcs-of-short-length-between-copper-electrodes [16].

Acknowledgements

This work was funded by the Deutsche Forschungsgemeinschaft (DFG) — project number 411446115.

References

[1] C. Uber, M. Hilbert, A. Felgner, et al. Electrical discharges caused by opening contacts in an ignitable atmosphere – part I: Analysis of electrical parameters at ignition limits. *J. Loss Prev. Proc. Ind.*, 61:114–121, 2019. doi:10.1016/j.jlp.2019.06.011.

[2] C. Uber, T. Runge, J. Brunzendorf, et al. Electrical discharges caused by opening contacts in an ignitable atmosphere – part II: Spectroscopic investigation and estimation of temperatures. *J. Loss Prev. Proc. Ind.*, 61, 2019. doi:10.1016/j.jlp.2019.05.010.

[3] R. Methling, S. Franke, C. Uber, et al. Optical emission spectroscopy of cadmium dominated discharges applied for assessment of explosion protection. *Plasma Phys. Technol.*, 10(1):47–51, 2023. doi:10.14311/ppt.2023.1.47.

[4] R. Shekhar, S. Gortschakow, H. Grosshans, et al. Numerical investigation of transient, low-power metal vapour discharges occurring in near limit ignitions of flammable gas. 52(4):045202, 2019. doi:10.1088/1361-6463/aaed04.

[5] M. J. Kushner. Modelling of microdischarge devices: plasma and gas dynamics. *J Phys D: Appl Phys*, 38(11):1633–1643, 2005. doi:10.1088/0022-3727/38/11/001.

[6] M. Baeva and D. Uhrlandt. Modelling of microarcs in copper metal vapour dominated air. *J. Phys. D: Appl. Phys.*, 58(9):095204, 2024. doi:10.1088/1361-6463/ad9f79.

[7] L. M. Biberman, V. S. Vorob'ev, , and I. T. Yakubov. Kinetics of impact-radiation ionization and recombination. *Sov. Phys. Usp.*, 15(4):375–394, 1973. doi:10.1070/PU1973v015n04ABEH004987.

[8] M. Baeva. Application of the transferred matrix method to a unified evaluation of the cathodic electron emission. *AIP Adv.*, 8(8):085322, 2018. doi:doi:10.1063/1.5041314.

[9] P. G. Slade. *The vacuum interrupter: Theory, design, and application*. CRC Press, 2008.

[10] B. J. McBride, M. J. Zehe, , and S. Gordon. NASA Glenn coefficients for calculating thermodynamic properties of individual species, NASA/TP-2002-211556. Technical report, NASA, Glenn Research Center, 2002.

[11] S. Stølen and F. Gronvøld. Heat capacity of solid cadmium from 298.15 to 594.22 K and of liquid cadmium from 594.22 to 700 K: enthalpy of fusion. 391:169–174, 2002.

[12] F. P. Incropera, D. P. DeWitt, T. L. Bergmann, and A. S. Lavine. *Fundamentals of heat and mass transfer*. Wiley, New York, USA, 2007.

[13] R. Honig. Rb-104: Vapor pressure data for the more common elements. Technical report, Radio corporation of America, RCA Laboratories, 1957.

[14] B. P. Marinkovic, R. P. McEachran, D. V. Fursa, et al. Cross sections for electron scattering from Cadmium: Theory and experiment. *J. Phys. Chem. Ref. Data*, 52:023102, 2023.

[15] Y. Raizer. *Gas Discharge Physics*. Springer, Berlin, 1991.

[16] M. Baeva, A. P. Jovanović, R. Methling, et al. Modelling microdischarges in metal vapour of cadmium - Dataset, 2025. doi:10.34711/INPTDAT.943.